Design of rectangular-groove fused-silica gratings as polarizing beam splitters

Qunyu Bi*, Jiangjun Zheng, Meizhi Sun, Fuling Zhang, Xinglong Xie, and Zunqi Lin

Shanghai Institute of Optics and Fine Mechanics, Chinese Academy of Science, Shanghai 201800, China
**luoxuele@gmail.com*

Abstract: The application of rectangular-groove fused-silica gratings as polarizing beam splitters (PBSs) under Littrow incidence is investigated. Based on the simple modal method, two different cases of PBS gratings are designed. The achieved solutions, which are independent on the incident wavelength, are verified by the rigorous coupled-wave analysis and expressed in several polynomials instead of listing one or two numerical solutions. More importantly, on the basis of the designed PBS gratings, a porous fused silica antireflective film is introduced to improve their performances. Theoretical results indicate that such modified rectangular-groove PBS gratings exhibit higher diffraction efficiencies (over 0.99) and larger spectral bandwidths.

OCIS codes: (050.1950) Diffraction gratings; (230.1360) Beam splitters; (230.5440) Polarization-selective devices; 240.0310) Thin films.

References and Links

1. H. Tamada, T. Doumuki, T. Yamaguchi, and S. Matsumoto, "Al wire-grid polarizer using the s-polarization resonance effect at the 0.8-μm-wavelength band," Opt. Lett. **22**(6), 419–421 (1997).
2. C. R. A. Lima, L. L. Soares, L. Cescato, and A. L. Gobbi, "Reflecting polarizing beam splitter," Opt. Lett. **22**(4), 203–205 (1997).
3. L. B. Zhou, and W. Liu, "Broadband polarizing beam splitter with an embedded metal-wire nanograting," Opt. Lett. **30**(12), 1434–1436 (2005).
4. R. C. Tyan, P. C. Sun, A. Scherer, and Y. Fainman, "Polarizing beam splitter based on the anisotropic spectral reflectivity characteristic of form-birefringent multilayer gratings," Opt. Lett. **21**(10), 761–763 (1996).
5. D. Yi, Y. B. Yan, H. T. Liu, S. Lu, and G. F. Jin, "Broadband polarizing beam splitter based on the form birefringence of a subwavelength grating in the quasi-static domain," Opt. Lett. **29**(7), 754–756 (2004).
6. S. Habraken, O. Michaux, Y. Renotte, and Y. Lion, "Polarizing holographic beam splitter on a photoresist," Opt. Lett. **20**(22), 2348–2350 (1995).
7. P. Lalanne, J. Hazart, P. Chavel, E. Cambril, and H. Launois, "A transmission polarizing beam splitter grating," J. Opt. A **1**, 215–219 (1999).
8. B. Wang, C. H. Zhou, S. Q. Wang, and J. J. Feng, "Polarizing beam splitter of a deep-etched fused-silica grating," Opt. Lett. **32**(10), 1299–1301 (2007).
9. H. T. Nguyen, B. W. Shore, S. J. Bryan, J. A. Britten, R. D. Boyd, and M. D. Perry, "High-efficiency fused-silica transmission gratings," Opt. Lett. **22**(3), 142–144 (1997).
10. J. Néauport, E. Journot, G. Gaborit, and P. Bouchut, "Design, optical characterization, and operation of large transmission gratings for the laser integration line and laser megajoule facilities," Appl. Opt. **44**(16), 3143–3152 (2005).
11. R. E. Collin, "Reflection and Transmission at a Slotted Dielectric Interface," Can. J. Phys. **34**, 398–411 (1956).
12. S. M. Rytov, "Electromagnetic Properties of a Finely Stratified Medium," Sov. Phys. JETP **2**, 466–475 (1956).
13. T. Clausnitzer, T. Kampfe, E. B. Kley, A. Tunnermann, U. Peschel, A. V. Tishchenko, and O. Parriaux, "An intelligible explanation of highly-efficient diffraction in deep dielectric rectangular transmission gratings," Opt. Express **13**(26), 10448–10456 (2005).
14. T. Clausnitzer, T. Kämpfe, E. B. Kley, A. Tünnermann, A. Tishchenko, and O. Parriaux, "Investigation of the polarization-dependent diffraction of deep dielectric rectangular transmission gratings illuminated in Littrow mounting," Appl. Opt. **46**(6), 819–826 (2007).
15. A. Drauschke, "Analysis of nearly depth-independent transmission of lamellar gratings in zeroth diffraction order in TM polarization," J. Opt. A **8**, 511–517 (2006).
16. L. F. Li, and C. W. Haggans, "Convergence of the Coupled-Wave Method for Metallic Lamellar Diffraction Gratings," J. Opt. Soc. Am. A **10**(6), 1184–1189 (1993).
17. M. G. Moharam, D. A. Pommet, E. B. Grann, and T. K. Gaylord, "Stable Implementation of the Rigorous Coupled-Wave Analysis for Surface-Relief Gratings - Enhanced Transmittance Matrix Approach," J. Opt. Soc. Am. A **12**(5), 1077–1086 (1995).

#124849 - $15.00 USD Received 16 Mar 2010; revised 15 Apr 2010; accepted 10 May 2010; published 21 May 2010

18. J. J. Zheng, C. H. Zhou, J. J. Feng, and B. Wang, "Polarizing beam splitter of deep-etched triangular-groove fused-silica gratings," Opt. Lett. **33**(14), 1554–1556 (2008).
19. Y. Ono, Y. Kimura, Y. Ohta, and N. Nishida, "Antireflection Effect in Ultrahigh Spatial-Frequency Holographic Relief Gratings," Appl. Opt. **26**(6), 1142–1146 (1987).
20. I. M. Thomas, "High laser damage threshold porous silica antireflective coating," Appl. Opt. **25**(9), 1481–1483 (1986).
21. P. F. Belleville, and H. G. Floch, "Ammonia-hardening of porous silica antireflective coatings," Proc. SPIE **2288**, 25–32 (1994).
22. C. Ballif, J. Dicker, D. Borchert, and T. Hofmann, "Solar glass with industrial porous SiO2 antireflection coating: measurements of photovoltaic module properties improvement and modelling of yearly energy yield gain," Sol. Energy Mater. Sol. Cells **82**(3), 331–344 (2004).
23. Y. Tang, H. Xiong, H. Li, and Z. Chen, "Preparation method for a porous SiO2 reducing film with controllable refractive index" (in Chinese) C.N. Patent (2009).
24. M. Krzyzak, G. Helsch, and G. H. Frischat, "Method of making a glass body with a phosphorous-and porous SiO2-containing coating, glass body made thereby and solution for making same," U.S.Patent (2006)
25. M. A. Golub, T. Hutter, and S. Ruschin, "Diffractive optical elements with porous silicon layers," Appl. Opt. **49**(8), 1341–1349 (2010).

1. Introduction

A polarizing beam splitter (PBS) is a key optical element that can split an incident wave into two orthogonally polarized beams. It is widely used in polarization-based imaging systems, free-space optical switching networks, magnetic-optic data storage systems, and so on. Conventional PBSs are usually designed on the basis of natural birefringence of crystals or multilayer dielectric coatings. Unfortunately, the commonly used crystals such as Nicol prisms and Wollaston prisms are heavy, bulky, expensive, and even worse, not easily integrated. As to the multilayer dielectric coating, it involves complicated fabrication process and suffers from a narrow-wavelength bandwidth.

Recently, the design of a simple subwavelength grating as a PBS in classical mounting has attracted great interest in that it cannot only solve problems of compactness inherent to the use of birefringent crystals, but also can be adapted to mass production in low cost. Taking advantage of different responses to the components of the incident light, a large number of PBS gratings have been designed. According to the splitting ways of the two orthogonally polarized optical fields, PBS gratings can be simply classified into: 1) both are reflected; 2) both are transmitted; and 3) one is reflected and the other is transmitted. In specific implementations, the realization of reflection usually requires the use of metal materials [1–3] or multilayer electric coatings [4], or involves some complicated structures [5]. However, the addition of metal materials in gratings not only increases the difficulty of PBSs design, but also arouses the absorption of incident radiation and the influence of heat transfer. With regard to the multilayer coating, its fabrication process is complicated and expensive. While designing an all-dielectric PBS grating to transmit both the polarized beams [6,7] could easily avoid the use of metal materials or multilayer coatings and the aforementioned troubles brought by them. Recently, Wang *et al.* reported an all fused-silica transmission grating as a broadband polarizer at the wavelength of 1550 nm, which were supposed to be used in optical communication [8]. Because of its compact structure and simple fabrication process, which only involves the employment of holographic recording technology and inductively coupled plasma etching to a monolithic fused silica plate, it is suitable for mass reproduction. Besides, due to the high laser damage threshold of fused silica, all fused-silica gratings can stand with high laser power [9,10]. Therefore, detailed investigation on the design of all fused-silica gratings as PBSs could be useful in a variety of practical applications.

The success of Wang's work [8] in developing the novel transmission PBS gratings has prompted us to further develop the grating structures and improve their performance. In this paper, we comprehensively investigate and modify the design of rectangular-groove fused-silica PBS gratings under classical light incidence. Firstly, we prove that the PBS gratings can be designed independently on the incident wavelength by varying the form of eigenvalue equation in the modal method developed by Collin *et al.* [11,12]. Secondly, based on the simple modal method (SMM) [13,14], the restrictions on grating structures to achieve two cases of PBS gratings are presented and their corresponding qualified structures are searched

#124849 - $15.00 USD Received 16 Mar 2010; revised 15 Apr 2010; accepted 10 May 2010; published 21 May 2010

out, respectively. Then through Lagrange interpolation of the results obtained by SMM, the quantitative relations among the structure parameters of the two sorts of devised PBS gratings are revealed in two polynomials, respectively, which are further verified by using rigorous coupled-wave analysis (RCWA). Finally but most importantly, on the basis of the designed PBS gratings, a porous fused silica antireflective film is successfully introduced to improve their properties. Theoretical results indicate that higher diffraction efficiencies and larger spectral bandwidths could be obtained in our modified rectangular-groove PBS gratings.

2. Designing principles and solutions

The schematic of fused-silica transmission PBS gratings with rectangular-groove is shown in Fig. 1, where the refractive indices of the air and the fused-silica substrate are n_1 and n_2, respectively; p is the grating period; d is the grating depth; the duty cycle f is defined as the ratio of the linewidth to period. The incident wavelength is λ and the incident angle is $\theta_{inc} = \sin^{-1}(\lambda/2n_1p)$, satisfying the Littrow condition in classical mounting. In Fig. 1(a), the TE (electric field vector parallel to the grating groove)- and TM(magnetic field vector parallel to the grating groove)-polarized waves are diffracted into the minus-first and zeroth orders, respectively, with diffraction angles $\theta_{-1} = \theta_0 = \sin^{-1}(\lambda/2n_2\, p)$ in the substrate. In Fig. 1(b), the TE- and TM-waves are diffracted into the zeroth and minus-first orders.

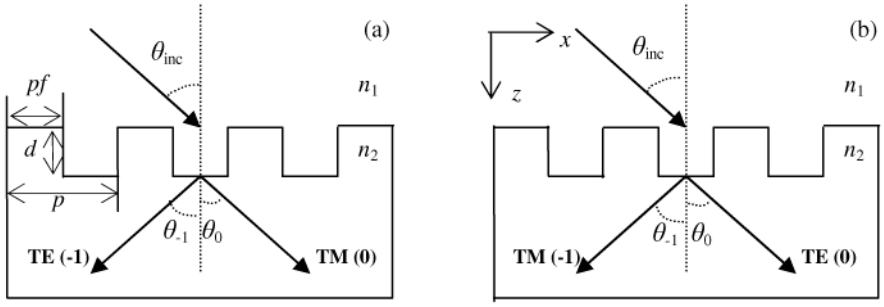

Fig. 1. Schematic of two polarizing split ways of transmission PBS gratings based on different designing principles: a) $\triangle n_{eff,TM} = 0$; b)$\triangle n_{eff,TE}/\triangle n_{eff,TM} = 2$.

In the modal method, the light in the grating is treated as a discrete set of modes. Their propagation constants are expressed by $k_z^m = k_0 n_{\text{eff}}^m$, where k_0 is the wave number of the incident light in air, k_z^m are the ones of diffractive beams in substrate, m indicates the order of modes. The effective indices n_{eff}^m satisfy the equation in the following

$$\cos(\frac{2\pi n_1 p \sin\theta_{\text{inc}}}{\lambda}) = F(n_{\text{eff}}^{m\,2}), \tag{1}$$

with

$$F(n_{\text{eff}}^{m\,2}) = \cos(\beta)\cos(\gamma) - \frac{1}{2}\xi \sin(\beta)\sin(\gamma), \tag{2}$$

where

$$\beta = \frac{2\pi pf}{\lambda}\sqrt{n_2^2 - n_{\text{eff}}^{m\,2}},$$

$$\gamma = \frac{2\pi p(1-f)}{\lambda}\sqrt{n_1^2 - n_{\text{eff}}^{m\,2}},$$

#124849 - $15.00 USD Received 16 Mar 2010; revised 15 Apr 2010; accepted 10 May 2010; published 21 May 2010

$$\xi = \begin{cases} \dfrac{\beta}{\gamma} + \dfrac{\gamma}{\beta} & \text{for TE-waves} \\ \dfrac{n_1^2 \beta}{n_2^2 \gamma} + \dfrac{n_2^2 \gamma}{n_1^2 \beta} & \text{for TM-waves} \end{cases}.$$

In the case of Littrow incidence, the left part of Eq. (1) becomes – 1, and its intersection with the right part of Eq. (1) leads to discrete values of n_{eff}^m. Only modes with $n_{\text{eff}}^m > 0$ can propagate along the *z*-direction. In order to show the relationship between n_{eff}^m and diffraction conditions more clearly, the form of Eqs. (1) and (2) are different with the ones in Refs [13,14]. Under the new form, it is easy to find that n_{eff}^m are related to the ratio of grating period to incident wavelength (*PVW*) instead of the concrete incident wavelength. In other words, the theoretical solutions of PBS gratings are applicable to different laser wavelengths and more information about the solutions would be useful for practical applications.

Although the exact calculation of diffraction efficiency of each order involves complicated computation of the overlap integral between the field of the incident wave and mode *m* at the air-grating boundary (Eq. (11) in Ref [13].), for deep etched fused silica gratings, Clausnitzer *et al.* [13,14] simplified the process into a two-beam interference of two propagating modes with different effective indices. The diffraction efficiencies of the minus-first and zeroth orders are only determined by accumulated phase difference $\Delta\varphi_{\text{polar}} = \dfrac{2\pi}{\lambda}\Delta n_{\text{eff,polar}} d$, where $\Delta n_{\text{eff,polar}}$ is the absolute value of $n_{\text{eff, polar}}^{-1} - n_{\text{eff, polar}}^{0}$, and the subscript, polar, identifies TE- or TM-waves. When $\Delta\varphi$ is even-numbered multiple of π, the zeroth order obtains the maximum energy; when it is odd-numbered multiple of π, the minus-first order does. Because TE- and TM-waves own different effective indices, it is possible to make the incident waves diffract into different orders by adjusting $\Delta\varphi$ through optimizing Δn_{eff} and grating depth.

2.1 The first polarizing split way

For TM-waves, there is an interesting phenomenon: for some particular gratings in a Littrow mounting, the grating depth exhibits little influence on diffraction efficiency of the zeroth transmitted order, which was revealed and discussed in Refs [12,15]. Actually, the phenomenon is the key to design PBS gratings and could be well explained by using SMM.

As expressed in Eq. (1), when the profile and materials of gratings are determined, the values of effective indices only relate to *PVW* and *f*. The solutions of Eq. (1) show that for some particular sets of *PVW* and *f*, $\Delta n_{\text{eff, TM}}$ equals to zero, but $\Delta n_{\text{eff, TE}}$ never does. That is why the phenomenon mentioned in Refs [12,15] was not observed under TE-waves illumination. Since $\triangle n_{\text{eff, TM}} = 0$, grating depth has no impact on the value of $\Delta\varphi$ and the zeroth order always obtain the maximum energy irrelevant to the grating depth.

#124849 - $15.00 USD Received 16 Mar 2010; revised 15 Apr 2010; accepted 10 May 2010; published 21 May 2010

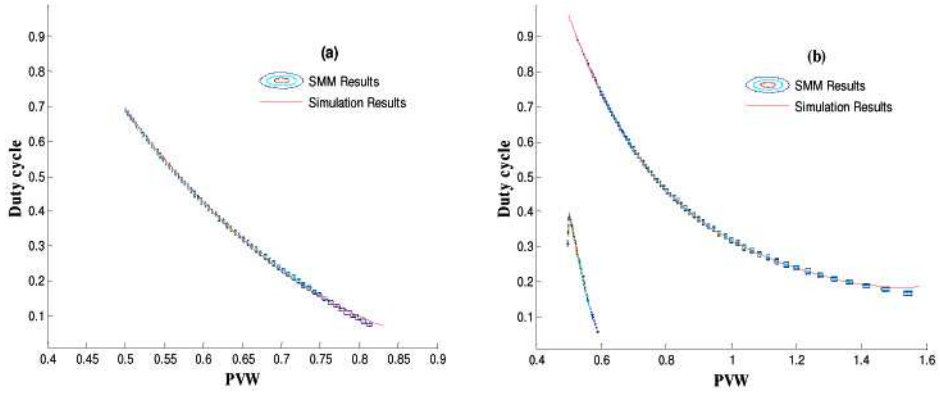

Fig. 2. Grating parameters (*PVW* and *f*) satisfying different designing principles for PBS gratings: a) $\triangle n_{\text{eff,TM}} < 0.001$; b) $1.98 < \triangle n_{\text{eff,TE}}/\triangle n_{\text{eff,TM}} < 2.01$.

With most energy of TM-waves in the zeroth order, setting proper grating depth to diffract most energy of TE-waves into the minus-first order will realize the function of a PBS. Then, setting the grating depth to make $\Delta\varphi_{\text{TE}}$ equal π, a PBS grating shown in Fig. 1(a) can be obtained. The contour lines in Fig. 2(a) sketch out the values of *PVW* and *f* satisfying $\triangle n_{\text{eff, TM}} < 0.001$. Their colors identify specific values of $\triangle n_{\text{eff, TM}}$. Because our purpose in this step is to search out the relation between *PVW* and *f*, the concrete values of $\triangle n_{\text{eff, TM}}$ are not shown. Using polynomial interpolation, the quantitative relations of *PVW*, *f*, and $\Delta n_{\text{eff, TE}}$ can be expressed as

$$f = 3.3098(PVW)^2 - 6.2731(PVW) + 2.991, \tag{3}$$

$$\Delta n_{\text{eff, TE}} = -1.9076 f^2 + 1.8060 f - 0.0214, \tag{4}$$

where *PVW* ranges from 0.5 to 0.8, and grating depth *d* is $\dfrac{\lambda}{2\Delta n_{\text{eff,TE}}}$. The red line in Fig. 2(a) is the fitting results described by Eq. (3), which is in accordance with the ones calculated by SMM. In order to check the performance of the PBS grating structures constrained by Eqs. (3) and (4), another well-developed and widely used tool for gratings design, RCWA, was adopted [16,17]. Figure 3(a) shows the calculated efficiencies (the zeroth order for TM-waves and the minus-first order for TE-waves) of the devised PBS gratings. Figure 3(b) illustrates the relevant top-part with supposed efficiencies both higher than 0.9 for TE- and TM-waves, which are all higher than the theoretical efficiency in Ref [8]. (0.8852 for TE-waves and 0.9862 for TM-ones). The reason that we present the solutions in polynomials is that it is useful for practical applications, and it is also the basis for the analyses of spectral bandwidths.

#124849 - $15.00 USD Received 16 Mar 2010; revised 15 Apr 2010; accepted 10 May 2010; published 21 May 2010

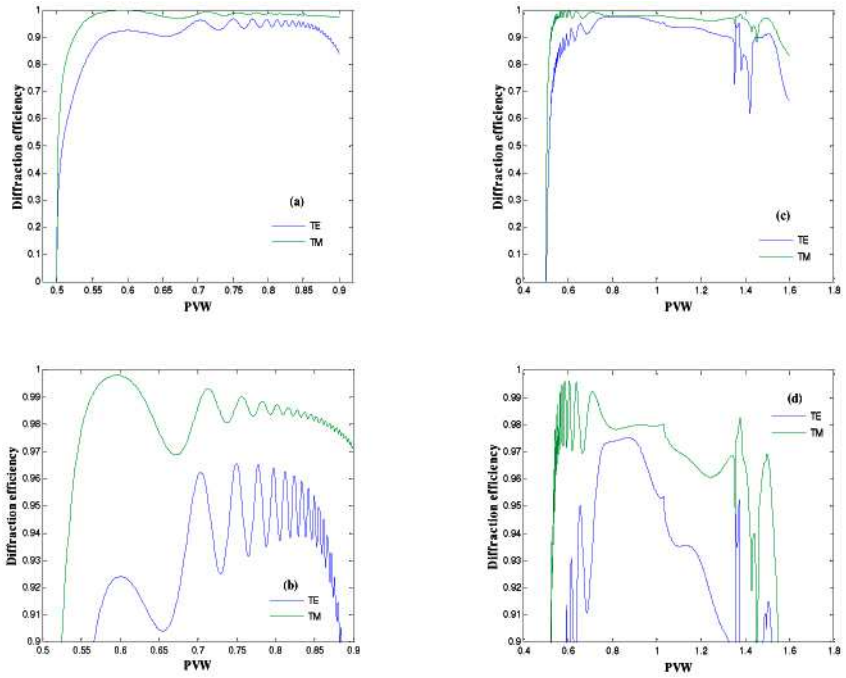

Fig. 3. Diffraction efficiencies of the supposed orders for gratings with different constructive parameters described by: (a) Eqs. (3) and (4); (b) Eqs. (5) and (6); (c) and (d) are partial enlarged detail with efficiencies larger than 0.9 of (a) and (b), respectively.

For practical applications, a broad wavelength range for the operation with broadband source is also very important. In PBS gratings design, Lalanne *et al.* defined extinction ratio to qualify the property [7]. The definition was also adopted in Ref [8]. and 89-nm spectral bandwidth (1512 – 1601 nm) was obtained with extinction ratios larger than 100. As for the result, there are two points need to be supplemented. One is that the result in Ref [8]. was obtained when the incident angle varies with the change of wavelengths (varied incident angle). When the angle is set only according to the central wavelength (constant incident angle), the spectral bandwidth should be 87 nm (within the range of 1514 – 1601 nm). Although it does not change a lot for the solution in Ref [8], the difference is quite obvious for our solutions. For example, the bandwidth is 77 nm (1507 – 1584 nm) for the constant incident angle, and 138 nm (1483 – 1621 nm) for the varied ones when $PVW = 0.7$ and $\lambda_0 =$ 1550 nm. Then it comes to the other point that different PBS gratings own different spectral bandwidths. As the energy is concentrated in the designed order, the efficiencies of the other orders is rather low and the extinction ratio is still high. Therefore, the spectral bandwidth is defined as the wavelength range with the concerned efficiencies both over 0.9 for our solutions. Although the spectral bandwidths varied greatly for different gratings, and we have not found out the relations between spectral bandwidths and grating structures, for specific gratings, the ratio of well-defined spectral bandwidth to incident wavelength is a constant. For instance, the largest spectral bandwidth under constant incident angle we could find occurs at $PVW = 0.731$. Its diffraction efficiency as a function of the ratio of incident wavelengths to the central wavelength is presented in Fig. 4(a). Two datatips illustrate that the spectral bandwidth is from $0.94\lambda_0$ to $1.047\lambda_0$ nm, where λ_0 is the central wavelength. When λ_0 equals 1550 nm, the corresponding spectral bandwidth should be 166 nm (1457 – 1623 nm).

#124849 - $15.00 USD Received 16 Mar 2010; revised 15 Apr 2010; accepted 10 May 2010; published 21 May 2010

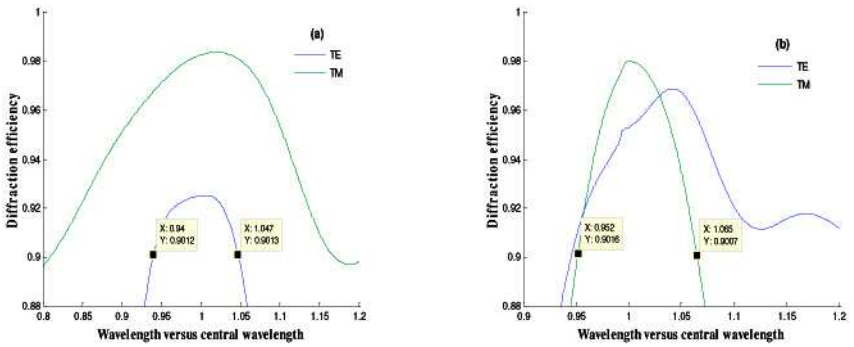

Fig. 4. Diffraction efficiency of the designed PBS gratings with the largest bandwidth under constant incident angle as a function of the ratio of wavelength to the central wavelength: a) *PVW* = 0.731 for the first polarizing split way; b) *PVW* = 1.03 for the second one.

2.2 The second polarizing split way

Since the purpose of PBSs is to split an incident wave into two orthogonally polarized beams, there is no reason for restricting on diffracting TE-waves into the minus-first order and TM-waves into the zeroth order. The reverse situation may also be considered, as shown in Fig. 1(b). According to the rules revealed by SSM, the corresponding requirement on grating structures is $\triangle n_{\mathrm{eff,TE}}/\triangle n_{\mathrm{eff,TM}} = 2$. The qualified *PVW* and f are shown in Fig. 2(b). Comparing with the first polarizing split way, the second method provides more structures to achieve PBS design. As shown in Fig. 2(b), the contour lines sketch out the region of *PVW* and f satisfying $1.98 < \triangle n_{\mathrm{eff,\,TM}}/\triangle n_{\mathrm{eff,\,TM}} < 2.01$, and two sets of interpolating polynomials are obtained. However, because the diffraction efficiencies of most gratings described by the shorter line are lower than 0.9, we only offer the polynomials of the longer one:

$$f = 1.0228(PVW)^4 - 5.1384(PVW)^3 + 10.0316(PVW)^2 - 9.2527PVW + 3.6559, \quad (5)$$

$$\Delta n_{\mathrm{eff,TE}} = -1.1568 f^2 + 1.0310 f + 0.1005, \quad (6)$$

where the range of *PVW* is 0.5 – 1.6, and the etching depth d equals to $\dfrac{\lambda}{\Delta n_{\mathrm{eff,TE}}}$. The red line in Fig. 2(b) is the fitting result, which is in accordance with the one calculated by SMM. The verified diffraction efficiencies of these PBS gratings are shown in Fig. 3(c), and the partial enlarged part with efficiencies more than 0.9 is shown in Fig. 3(d). When *PVW* is larger than 1.35, the propagating modals are over two and SMM is no longer applicable.

Comparing the results of the two polarizing split ways illustrated in Figs. 3(b) and 3(d), it is obvious that the diffraction efficiencies of the second polarization method are higher for *PVW* in the range of 0.7 – 1, which are all over 0.97 and no oscillation. However, it also required deeper etching depth, about three times of incident wavelength, compared with two times of incident wavelength (the smallest is 1.7 times of incident wavelength) for some solutions of the first polarizing split way. As to the spectral bandwidth shown in Fig. 4(b), the largest bandwidth of the second method appears higher ($0.1130\lambda_0$ for the second method and $0.1070\lambda_0$ for the first one).

3. Improved rectangular-groove PBS gratings

Although the diffraction efficiency could be improved to some extent by using the second polarizing split way, it requires deeper etching depth and there still are more than about 0.2 loss of energy. The introduction of a triangular-groove PBS grating proved that the efficiencies could be improved [18]. Further analysis on the structure indicate the reason that triangular-groove gratings can achieve higher maximum diffraction efficiency is its

#124849 - $15.00 USD Received 16 Mar 2010; revised 15 Apr 2010; accepted 10 May 2010; published 21 May 2010

antireflection effect [19], which lead us to assume that any method that can reduce reflection might benefit to improve diffraction efficiencies. Because it is more difficult to fabricate gratings with triangular-groove than those with rectangular-groove, we limit that the grating groove is rectangular and attempt to find other methods to reduce reflection.

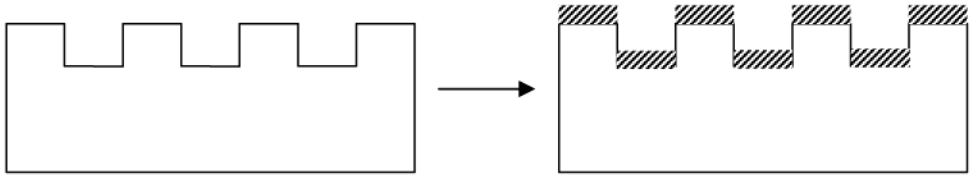

Fig. 5. Schematic of an improved PBS grating from an original one with rectangular- groove.

When it comes to reducing reflection, one of the most common ways is coating reflection reducing film. The use of porous silica as an antireflective coating is well developed and many fabrication methods have been introduced. With different technologies for the preparation of porous silica layers, such as acid etching of the glass, sol-gel deposition, direct plasma enhanced chemical vapor deposition, and so on, the refractive index of fused-silica can be adjusted from 1.22 to 1.29 [20–25]. Therefore, we decide to apply porous silica as an antireflective coating on the top of the designed PBS gratings mentioned above to improve their properties. A schematic of an improved PBS grating from an original one is shown in Fig. 5, where the shadow part represents a porous fused-silica reducing film. Its antireflection effect depends on both refractive index and thickness of the film. For simplicity, the refractive index is set to 1.23, and only the thickness is optimized. With the criterion that improving the efficiencies of the greatest number of gratings, the thickness is set to $0.2581\lambda_0$.

Figure 6 illustrate the efficiencies of the PBS gratings after adding the antireflective film, whose profile parameters are still the same ones designed in Sections 2.1 and 2.2. Comparing Fig. 3(b) with Fig. 6(a), and Fig. 3(d) with Fig. 6(c), respectively, the maximum diffraction efficiencies are increased from 0.96 to 0.99 for the first polarizing split way, and from 0.97 to 0.99 for the second one. The efficiency oscillation in Fig. 3(b) is also obviously reduced. The grating structures that can achieve high efficiencies are also greatly enlarged. For the first polarizing split way, the grating structures with *PVW* ranging from 0.582 to 0.854 could all reach the designed efficiencies over 0.99; for the second one, the *PVW* ranges from 0.624 to 1.049. Besides, the efficiencies of the structures visualized by the shorter line in Fig. 2(b) also rise, as shown in Fig. 6(d), but the thickness of the film changes to $0.3548\lambda_0$.

#124849 - $15.00 USD Received 16 Mar 2010; revised 15 Apr 2010; accepted 10 May 2010; published 21 May 2010

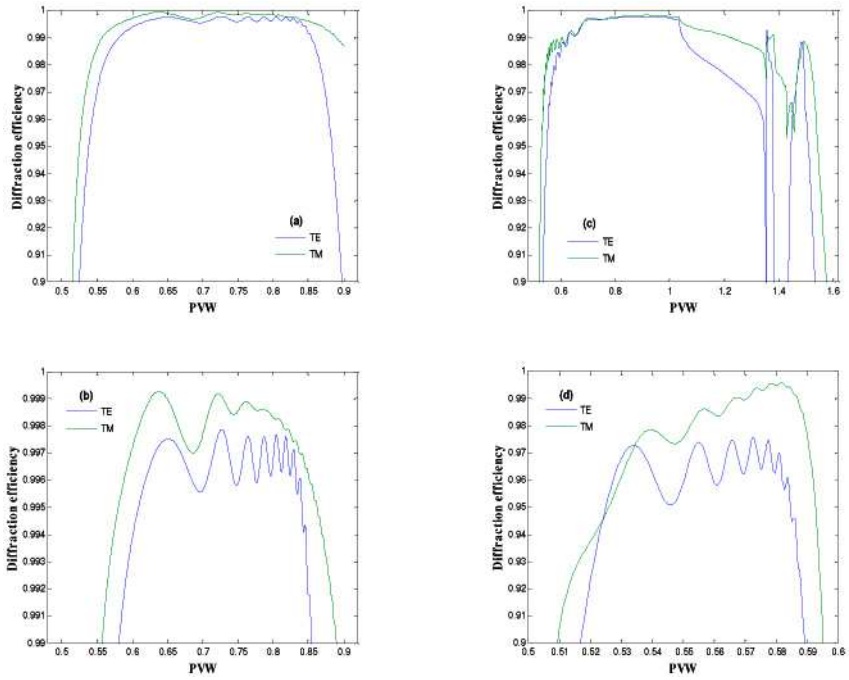

Fig. 6. Diffraction efficiencies of the supposed orders for improved PBS gratings with different constructive parameters described by: (a) Eqs. (3) and (4); (c) Eqs. (5) and (6); (d) the shorter line in Fig. 2(b); (b) is the partial enlarged detail with efficiencies larger than 0.99 of (a).

The addition of the antireflection film on the surface of the rectangular-groove gratings not only increases diffraction efficiencies markedly, but also does the spectral bandwidth. Similar to the original PBS gratings, the maximal spectral bandwidths for the improved PBS gratings are represented in Fig. 7, which are improved from $0.1070\lambda_0$ to $0.1602\lambda_0$ for the first method and $0.1130\lambda_0$ to $0.1376\lambda_0$ for the second one.

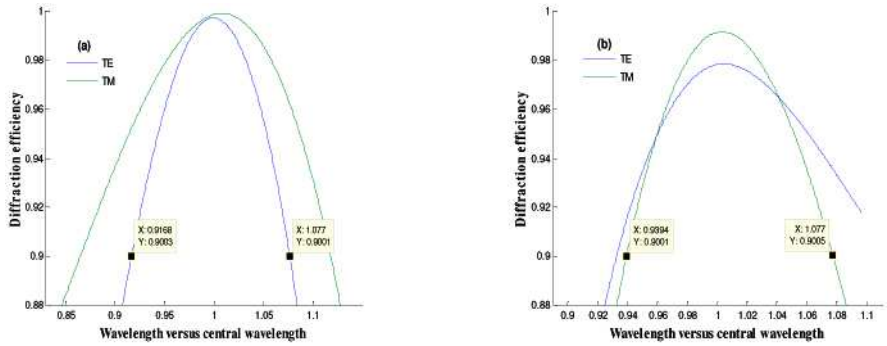

Fig. 7. Diffraction efficiency of the improved PBS grating with the largest bandwidth under constant incident angle as a function of the ratio of wavelength to the central wavelength: a) $PVW = 0.655$ for the first polarizing split way; b) $PVW = 1.18$ for the second one.

For a triangular-groove PBS grating in Ref [18], its efficiencies were higher than 0.96 in a band range of 1480 – 1620 nm for both TE- and TM- polarizations, and over 0.99 for the central wavelength, when p = 900 nm and d = 2966 nm. Our results show that for varied incident angle, the designed efficiencies are over 0.90 for wavelength varying from 1399 to 1668 nm, and from 1444 to 1644 nm for constant incident angle. For our improved gratings, the spectral bandwidth also varies obviously with the grating structures. For the first polarizing split way, the maximum bandwidths are 248 nm (1421 – 1669 nm) for constant

#124849 - $15.00 USD Received 16 Mar 2010; revised 15 Apr 2010; accepted 10 May 2010; published 21 May 2010

incident angle, and 367 nm (1369 – 1736 nm) for varied incident angle. The corresponding values are 214 nm (1456 – 1670 nm) and 261 nm (1442 – 1703 nm) for the second polarizing split way. Therefore, the largest spectral bandwidth of modified fused-silica rectangular-groove PBS gratings are similar to that of triangular-groove PBS gratings.

5. Conclusion

We have presented the design of fused-silica rectangular-groove PBS gratings in classical Littrow mounting, and introduced a simple method to improve their properties. According to different requirements on grating parameters (one is $\triangle n_{\text{eff, TM}} = 0$ and the other one is $\triangle n_{\text{eff, TE}}/\triangle n_{\text{eff, TM}} = 2$), two different cases of PBS gratings are designed and discussed, respectively. The quantitative relation among PBS grating parameters are revealed in four polynomials. Furthermore, based on these achieved structures, we introduce a porous fused-silica film to reduce their reflection effect and greatly improve their properties. Theoretical results prove that the diffraction efficiencies are significantly improved for most grating structures (over 0.99 with *P*VW ranging from 0.582 to 0.854 for the first polarizing split way, and from 0.624 to 1.049 for the second one), as well as the largest spectral bandwidth (from $0.1070\lambda_0$ to $0.1602\lambda_0$ for the first polarizing split way and from $0.1130\lambda_0$ to $0.1376\lambda_0$ for the second one). Because the designed gratings parameters are denoted in simple polynomials and valid for different wavelengths just by simply scaling the parameters, the structure parameters of a desired PBS grating suitable to various specific situations can be easily determined without complicated calculation. However, the actual performance of PBS gratings depends greatly on fabrication technique, and their fabrication tolerance varied with the devised grating parameters and the wavelength of incident light, which require to be discussed in concrete situations and further research in the future.

Acknowledgements

This work was supported by the National High Technology Research and Development Program of China under Grant No. 2009AA8044010.

#124849 - $15.00 USD Received 16 Mar 2010; revised 15 Apr 2010; accepted 10 May 2010; published 21 May 2010